Calculations of rate constants for reactions of first and second row cations

A.I. González[1*], **D.C. Clary**[1], **M. Yáñez**[2]

[1]Department of Chemistry, University College of London, 20 Gordon Street, London WC1H OAJ, UK
[2]Department of Chemistry, C-9, Universidad Autónoma de Madrid, Cantoblanco, E-28049 Madrid, Spain

Abstract. Calculations of rate constants for 35 reactions of first and second row monocations with different neutrals are presented. A combined rotationally adiabatic capture and centrifugal sudden approximation is used. The majority of predicted rate constants are in good agreement with the experimental measurements. An exploration of energetics of the potential energy surface for some of those cases in which prediction fails has been done using ab initio G2 theory. These cases usually correspond to situations in which the reaction is not as exothermic as the application of capture approximation requires or secondary barriers exist in the reaction path. Second row cations present these kind of problems due to their smaller electronegativity with respect to cations of the first row.

Key words: Rate constants – Cation reactions – Adiabatic capture

1 Introduction

Ion gas-phase chemistry has been an area of major interest and growth in recent years [1]. Theoreticians and experimentalists have paid special attention to this subject, mainly due to its well-known importance in plasma, atmospheric, interstellar and circumstellar chemistry [2]. In the experimental field several techniques have been developed to study different aspects of ion gas-phase reactions. Improvements, mainly in high-resolution ion spectroscopy [3] and mass spectrometry [4], have made it possible to carry out accurate measurements, overcoming the intrinsic difficulties of working with such highly reactive systems. Nevertheless, in spite of widespread technological improvements, the experimental determination of magnitudes such as rate

coefficients is still arduous. Only a small number of ion-molecule systems relevant to interstellar chemistry have been investigated experimentally, although reliable temperature-dependent rate constants are crucial to perform simulations of chemical synthesis in different interstellar media. Therefore, theoretical calculations play an important role in producing many of the required constants, as well as in the fundamental understanding of ion-molecule reaction.

From the theoretical point of view, the development of ab initio methods allows energies, structures and vibrational frequencies to be calculated quite reliably. In this sense a vast amount of information about thermodynamic aspects of this kind of systems has been reported; however, the available information on dynamics is still rather scarce. Several theories have been elaborated to describe chemical reactions; many of these theories are based on rigorous quantum mechanics and are usually applied to systems with barriers in the potential energy surface [5]. In this paper we are interested in the so-called fast reactions [6]. These reactions have rate constants that may be orders of magnitude larger than those corresponding to reactions with a barrier. An usually common characteristic of these systems is that the rate constants are dominated by the long-range part of the potential. This fact makes possible two important simplifications; in the first place, it is reasonable to assume a classical capture approximation, i.e. a reaction will occur if there is enough translational energy along the reaction coordinate to overcome the centrifugal rotational barrier. Secondly, it is not necessary to solve the Schrödinger equation over the whole space, but only in the long-range part of the entrance channel to the reaction, where the potential could be accurately described in terms of multipolar moments and other molecular properties. Considering these two premises, a large number of approximate theories have been proposed for ion-dipole reactions [7]. In the present study we employ a method which combines a rotationally adiabatic capture and centrifugal sudden approximation (ACCSA) [8, 9]. This method has been applied successfully in previous studies [10–12] not only for ion-dipole systems, but also for some molecule-molecule reactions involving both

---

Permanent address: Department of Chemistry, C-9, Universidad Autónoma de Madrid, Cantoblanco, E-28049 Madrid, Spain
Correspondence to: A.I. González

ions and neutrals [8]. This approach is particularly accurate for reactions involving proton transfer [13], which are especially suitable for this method because they are strongly exothermic reactions with no secondary barriers in the potential energy surface. These characteristics make it possible to neglect the probability of reflection of reactive flux through the centrifugal barrier.

Our main goal in this work is to calculate global rate constants for a large number of ion-dipole systems for which experimental information is available. The objective is to test the method for reactions of a wide number of cations (not only from the first row, but also from the second row) with different neutrals. In some cases in which we have found disagreement between theory and experiment we have used ab initio calculations to explore the energetics of the potential energy surface in order to determine the causes of this disagreement. Some of these hypersurfaces, mainly those corresponding to systems of small size, have been reported previously in the literature; some others have been calculated, totally or partially, in this work.

2 Computational details

2.1 ACCSA method

In this section we outline the main features of the ACCSA method. The reader can find a more complete description in Refs. [8–10].

As stated in Sect. 1, the ACCSA method is suitable for systems in which the long-range intermolecular forces are dominant, for instance, strongly exothermic reactions with no barrier in the potential energy surface. The intermolecular potential in the long-range region can be described as follows:

$$V(R, \theta) = -\alpha q^2/2R^4 - q\mu_D \cos\theta/R^2$$

where $\mathbf{R}$ is the vector between the ion and the centre of mass of the molecule, μ_D is the dipole moment, α is the isotropic polarizability, q is the charge on the ion and θ is the angle that $\mathbf{R}$ makes with the direction of the molecular dipole.

The use of this potential is not a necessary constraint in the ACCSA method. Any other suitable potential, for instance any potential obtained with ab initio methods, can be used, providing it can be expanded in terms of a Legendre series in $\cos\theta$.

The Hamiltonian for the entrance channel, written in body-fixed coordinates, is:

$$H = H_{\rm rot} - \frac{1}{2\mu R}\frac{\partial^2}{\partial R^2}R + \frac{|\mathbf{J} - \mathbf{j}|^2}{2\mu R^2} + V(R, \theta)$$

where $\mathbf{j}$ is the rotational momentum of the molecule and $\mathbf{J}$ is the total angular momentum for the ion-molecule system, and μ is the reduced mass of the collisional system.

If we assume the centrifugal sudden approximation, we can replace $|\mathbf{J} - \mathbf{j}|^2$ by the diagonal value $[J(J+1) + \mathbf{j}^2 - 2\Omega^2]$. With the potential given, depending only on R

and θ, this approximation eliminates the coupling between states of different Ω (the projection quantum number for both $\mathbf{J}$ and $\mathbf{j}$ along the body-fixed Z-axis).

In this study we have considered the molecule as a symmetric top for which $H_{\rm rot}$ is given by:

$$H_{\rm rot} = B\mathbf{j}^2 + (A - B)\mathbf{j}_z^2$$

Diagonalization of H over a range of fixed R values yields the rotationally adiabatic potential-energy curves $\{\varepsilon_{jK\Omega}(R)\}$, where the j, K and Ω labels refer to the quantum numbers of the asymptotic state.

To calculate the reaction cross-sections, the capture approximation is applied: the reaction probability is unity if the collision energy is above the centrifugal barrier and zero if it is below. This approximation enables us to obtain capture cross-sections, state-selected in j and K, for an appropriate range of collisional energies. Maxwell-Boltzman averaging over this grid of energies yields the state-selected rate constants, $k_{jK}(T)$, and finally averaging again over the initial rotational states we have the global rate constants, $k(T)$. In our case the global rate coefficients are reported at 300 K as the experimental values available are given at this temperature.

Although the ACCSA method provides valuable information about state-selected cross-sections and rate constants as functions of the temperature, our main goal here is to calculate global rate constants for a large number of ion-dipole systems for which experimental data have been reported. In any case this information (state-selected cross-sections and rate constants as functions of the temperature) is available from the authors upon request.

The main advantages of this simple method are its low computational cost and its general applicability. For ion-molecule systems, the only parameters needed are the ion charge and some molecular properties (dipole moment, polarizability, mass and rotational constants).

2.2 Ab initio calculations

As mentioned above, in some specific cases where a significant disagreement was found between the experimental rate constant and our theoretical estimation, we have explored the energetic characteristics of the potential energy surfaces along the reaction path by using ab initio molecular orbital calculations. More specifically, we have done this study for the $O^+(^4S) + NH_3$ and $N^+(^3P) + NH_3$ systems and we have also calculated some stationary points of the $C^+ + H_2O$ surface in order to complete the reaction profile since, as we will see, the $[C, H_2, O]^+$ system has been studied before. In all cases the geometries of the structures involved were optimized at the MP2/6-31G* level. In order to obtain as reliable energetics as possible, the total energies were determined in the framework of the G2 theory [14]. G2 theory is a composite procedure based on Møller-Plesset perturbation theory at second and fourth orders (MP2 and MP4) and quadratic configuration interaction including single, double and triple excitation QCISD(T) levels of theory. Assuming additivity of different basis set enhancements

at the MP4 level and additivity of basis set and correlation effects between MP4 and QCISD(T), a total energy effectively of a QCISD(T)/6-311+G($3df, 2p$) quality is obtained. Frequency calculations were carried out at MP2 level and zero point energies were then scaled by the empirical factor 0.93.

All these calculations were performed using the Gaussian-94 series of programs [15].

3 Results and discussion

We have applied the theory described above to systems constituted by first and second row monocations ($C^+, N^+, O^+, F^+, Si^+, P^+, S^+, Cl^+$) and different neutrals ($NH_3, H_2O, CH_3OH, H_2CO, H_2S, HCOOH$).

Table 1 shows the molecular parameters used to build the potential for each case. Ab initio calculations sometimes yield molecular properties such as dipole moments and polarizabilities affected by large errors so we have employed the experimental values [16] for both these properties. Rotational constants were obtained from the corresponding optimized geometries at the MP2/6-31G* level. In this respect it has been shown [10] that for temperatures of 300 K and below, the K projection quantum number usually does not have an important effect on the reaction rate constant. Hence, we have considered it reasonable to treat neutrals that are not rigorously symmetric top molecules as if they were by averaging the asymmetric top constants B and C.

In Table 2 we compare the experimental values of the rate coefficients taken from Ref. [17] with our calculated values. We also show the experimentally detected products.

For a majority of reactions we find a good agreement between experimental and theoretical rate constants, with differences lower than 20%, which is the experimental uncertainty assumed in most cases. When we find disagreement we appreciate an overestimation of the rate constant with respect to the experimental one in all cases but for the $N^+ + HCOOH$ and $O^+ + HCOOH$ reactions. The aforementioned overestimation is an expected result if we consider that all the approximations in our method tend to yield an upper bound of the rate constant. On the one hand, when the capture sudden approximation is used we are not taking into account the probability of flux going back through the entrance channel. Hence, if high barriers prevent the dissociation of the collision complex into products it is possible that reaction could be slowed down. On the other hand, the

existence of repulsive excited state potential energy surfaces that are degenerated on the reactant side may also lead to rate constants lower than the estimated ones [18]. In these cases we can apply a statistical factor f that stands for the fraction of attractive potential energy surfaces in such a way that the rate constant has a value between the capture constant and the capture constant multiplied by f ($k_c > k > fk_c$).

In summary, according to these arguments, in general, it is very unlikely to obtain theoretical values below the experimental ones by using the ACCSA method and therefore we suggest it would be desirable to revise the experimental rate coefficients reported for the $N^+ + HCOOH$ and $O^+ + HCOOH$ reactions.

The analysis of reaction paths may be helpful in rationalizing those cases in which we found disagreement. Many of these surfaces have been studied before and have been reported in the literature, especially for those cases where the size of the species involved allows an ab initio treatment; we will make use of some of them in our discussion. In other cases, where this information was not available or was incomplete, we have explored the characteristics of the stationary points along the reaction path using the methods described in the section on computational details.

The first finding that attracted our attention was the remarkable disagreement between theoretical and experimental rate constants found in the case of Si^+ reactions when the neutrals are NH_3 and H_2O, while for the other cation of the same group, C^+, the agreement is reasonably good. The dynamics of the reaction $Si^+ + NH_3$ has already been studied by Flores et al. [19] by means of an approximate classical trajectory method and RRKM theory and therefore will not be discussed in detail here. Briefly, the conclusions of this study indicate that $Si^+ + NH_3$ is a reaction in which there are repulsive PES degenerated on the reactant side and also high energetic barriers in the dissociation channels of the collision complex. These are the reasons why their estimated capture constant at 300 K has a value of $2.03 \times 10^9 \, cm^3 \, s^{-1} \, molec^{-1}$ while the bimolecular value is found to be $0.66 \times 10^{10} \, cm^3 \, s^{-1} \, molec^{-1}$, i.e. approximately one third of the capture constant.

Related to the $Si^+ + H_2O$ reaction, the thermochemical stabilities of the isomers of $[H_2, Si, O]^+$ have been reported [20]. We have found it interesting to compare this reaction with its analogous $C^+ + H_2O$. The hypersurface $[H_2, C, O]^+$ has been described in Refs. [21, 22]. There the main goal was the study of rearrangement and dissociative processes associated with formaldehyde and methanol cations respectively. We have used this information to construct the reaction profile of $C^+ + H_2O$, calculating the stationary points needed to complete this profile at the G2 level of theory, the same level employed in Ref. [22].

In Fig. 1 we can see that reaction paths are similar in both cases, with minor differences. Although the surfaces have been calculated at different levels of theory it is reasonable to assume, due to the quality of both calculations, that there must not be qualitative differences and the quantitative changes will be small. In these reactions the first step is the formation of the adduct

Table 1. Molecular parameters. Polarizability[a] (Å^3), dipole moment[a] (D), rotational constants[b] (cm^{-1})

	NH$_3$	H$_2$O	CH$_3$OH	H$_2$CO	H$_2$S	HCOOH
α	2.26	1.45	3.29	2.45	3.80	4.42
μ	1.47	1.85	1.70	2.33	0.97	1.41
A	6.31	26.50	4.25	9.58	10.5	2.34
B	9.85	11.84	0.81	1.19	6.81	0.38

[a] Experimental values
[b] Corresponding to the optimized geometries at the MP2/6-31G* level

Table 2. Experimental[a] and calculated rate coefficients ($\times 10^{-9}\,\mathrm{cm^3\,s^{-1}}$; T = 300 K); experimentally detected reaction products

|		NH$_3$	H$_2$O	CH$_3$OH	H$_2$CO	H$_2$S	HCOOH
C$^+$	K$_{exp}$(T)	2.3	2.4	3.4	4.2	1.8	3.3
	K$_{calc}$(T)	2.7	2.8	3.5	3.8	2.2	3.3
	Products	NH$_3^+$ + C(0.32) HCN$^+$ + H$_2$(0.05) HCNH$^+$ + H(0.63)	H$_2$O$^+$ + C(0.10) HOC$^+$ + H(0.90)	CH$_3^+$ + HCO(0.80) CH$_2$OH$^+$ + CH (0.20)	CH$_2^+$ + CO(0.54) HCO$^+$ + CH(0.20) H$_2$CO$^+$ + C(0.26)	H$_2$S$^+$ + C(0.27) HCS$^+$ + H(0.73)	HCO + HCO$^+$(1.00)
Si$^+$	K$_{exp}$(T)	0.64	0.23	2.2			2.3
	K$_{calc}$(T)	2.2	2.3	2.7			2.4
	Products	SiNH$_2^+$ + H(1.00)	SiOH$^+$ + H(1.00)	SiOH$^+$ + CH$_3$(0.75) SiOCH$_3^+$ + H(0.25)			SiOH$^+$ + HCO (1.00)
N$^+$	K$_{exp}$(T)	2.4	2.7	3.1	2.9	1.9	6.2
	K$_{calc}$(T)	2.6	2.7	3.3	3.6	2.0	3.1
	Products	NH$_2^+$ + NH(0.20) NH$_3^+$ + N(0.71) N$_2$H$^+$ + H$_2$(0.09)	H$_2$O$^+$ + N(1.00)	CH$_3$OH$^+$ + N($\approx$ 0.40) H$_2$CO$^+$ + NH$_2$ ($\approx$ 0.30)	HCO$^+$ + NH(0.25) H$_2$CO$^+$ + N($\approx$ 0.65) NO$^+$ + CH$_2$($\approx$ 0.10)	NH$^+$ + SH(0.03) S$^+$ + NH$_2$(0.12) HS$^+$ + NH(0.29) H$_2$S$^+$ + N(0.56)	HCO$^+$ + HNO (1.00)
P$^+$	K$_{exp}$(T)	2.0	0.55	1.4		1.4	
	K$_{calc}$(T)	2.2	1.9	2.6		1.6	
	Products	NH$_3^+$ + P(0.52) NHP$^+$ + H$_2$(0.01) NHPH$^+$ + H(0.48)	PO$^+$ + H$_2$(0.09) POH$^+$ + H(0.91)	POH$^+$ + CH$_3$(1.00)		H$_2$S$^+$ + P(0.31) PS$^+$ + H$_2$(0.12) HPS$^+$ + H(0.57)	
O$^+$	K$_{exp}$(T)	1.2	2.6	1.9	3.5	1.9	5.0
	K$_{calc}$(T)	2.5	2.6	2.8	3.5	2.0	2.9
	Products	NH$_3^+$ + O(1.00)	H$_2$O$^+$ + O(1.00)	H$_2$CO$^+$ + H$_2$O(0.05) CH$_2$OH$^+$ + O(0.70) CH$_2$OH$^+$ + O(0.25)	HCO$^+$ + OH(0.40) H$_2$CO$^+$ + O(0.60)	S$^+$ + H$_2$O(0.11) HS$^+$ + OH(0.21) H$_2$S$^+$ + O(0.68)	HO$_2^+$ + HCO HCO$^+$ + HO$_2$
S$^+$	K$_{exp}$(T)	1.5	No reaction		0.67	0.82	
	K$_{calc}$(T)	2.2			2.8	1.6	
	Products	NH$_3^+$ + S(0.92) NHSH$^+$ + H(0.08)			H$_2$S$^+$ + CO(0.50) HCO$^+$ + SH(0.50)	S$_2^+$ + H$_2$(0.70) S$_2$H$^+$ + H(0.23) S$_2$H$_2^+$ + $h\mu$(0.06)	
F$^+$	K$_{exp}$(T)	2.1	3.1			0.76	
	K$_{calc}$(T)	2.4	2.5			1.8	
	Products	NH$^+$ + HF + H(0.05) NH$_2^+$ + HF(0.79) NH$_3^+$ + F(0.12) HF$^+$ + NH$_2$(0.04)	O$^+$ + HF + H(0.17) OH$^+$ + HF(0.06) H$_2$O$^+$ + F(0.66) HF$^+$ + OH(0.11)			S$^+$ + HF + H(0.16) HS$^+$ + HF(0.84)	
Cl$^+$	K$_{exp}$(T)	0.78	0.50			1.6	
	K$_{calc}$(T)	2.1	2.2			1.5	
	Products	NH$_2^+$ + HCl(0.04) NH$_3^+$ + Cl(0.96)	H$_2$O$^+$ + Cl(1.00)			H$_2$S$^+$ + Cl(0.63) HS$^+$ + HCl(0.28) HCl$^+$ + SH(0.09)	

[a] Experimental results taken from ref. [15]

corresponding to the association of the cation with the oxygen atom of the water molecule. The complex could evolve through the transition state TS1/2 to the insertion of the cation into the O—H bond or through the transition state TS 1/d to the dissociation into H + XOH$^+$ fragments ($X = $ C, Si). From complex 2 or its *cis*-isomer, 3, the reaction results in the loss of *H*. For Si$^+$ the only possibility found is the fission of the Si—H bond without any barrier. For C$^+$ the same possibility exists but it is also possible to break the O—H bond through TS 2/d and TS 3/d respectively. In this case the experimentally detected products could probably be a mixture of

HCO$^+$/COH$^+$ isomers, as all the mechanisms are energetically allowed, although formation of HCO$^+$ seems to be a more competitive process. It is noteworthy that the products corresponding to the charge transfer process are predicted to be 33.6 kcal/mol above the entrance channel. This suggests that the small ratio of products experimentally detected corresponding to the charge transfer process might be a consequence of an excess of kinetic energy in the colliding particles.

More relevant to our discussion is the importance of energetic barriers in the mechanisms. While for C$^+$ + H$_2$O the higher barrier in the path is about 55 kcal/

Fig. 1. Energetic profile for the C$^+$(^{2}P) + H$_2$O and Si$^+$(^{2}P) + H$_2$O reaction paths
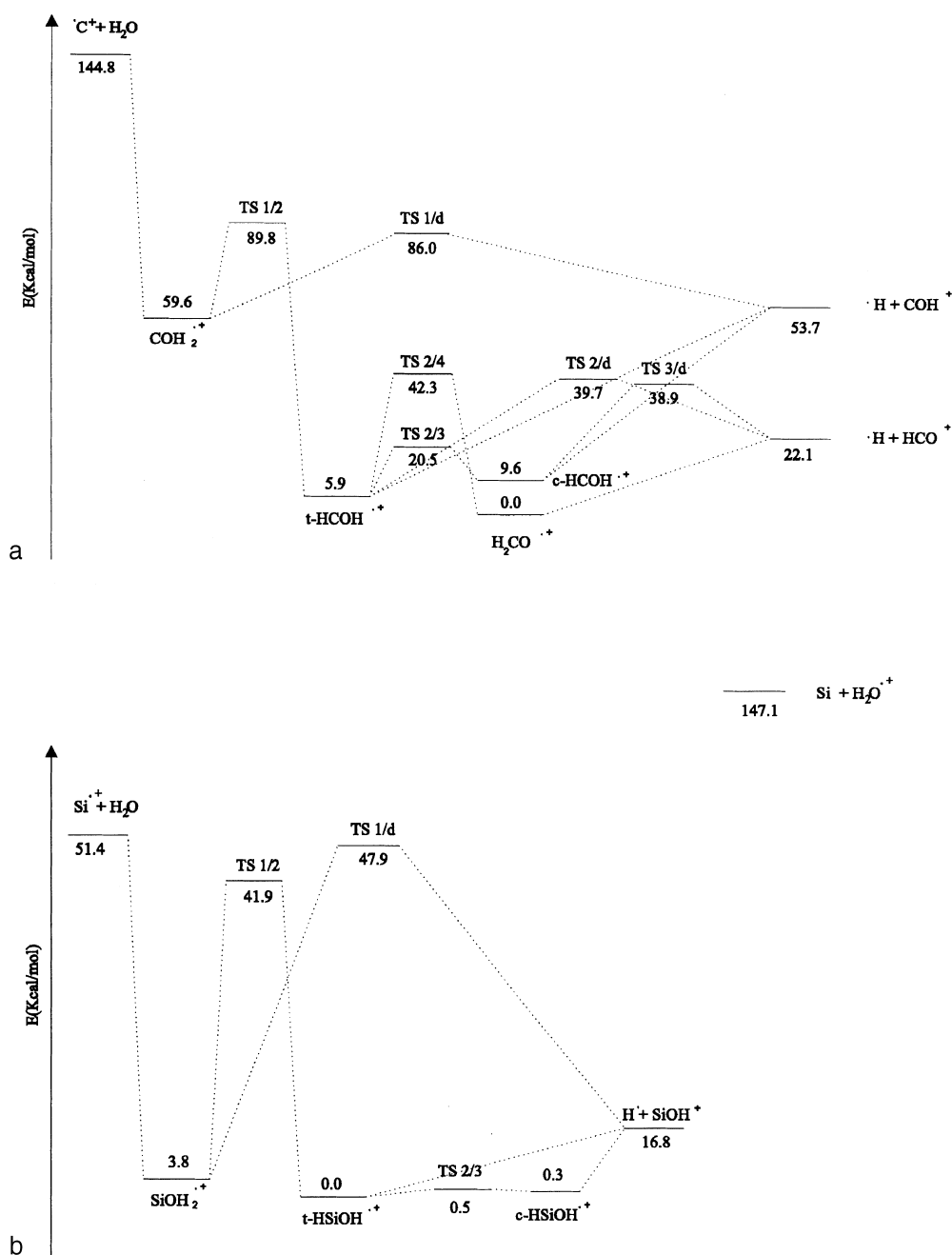
mol below the reactants, in the case of $Si^+ + H_2O$ there are important barriers for both possible mechanisms, which are only about 10 and 3.5 kcal/mol below the entrance channel. Therefore $Si^+ + H_2O$ is not such a good candidate for application of the capture approximation.

This is also the case for $P^+ + H_2O$; this reaction has been studied in Ref. [23], both energetically and dynamically, employing the same method used in Ref. [19]. In this study they found only moderate agreement of the computed bimolecular rate coefficient when a factor of 1/3 (which represents the fraction of attractive degenerate electronic states of the reactants at infinite separation) is used to correct the capture rate. This may be due once again to the presence of high barriers [23] in the

reaction profile that make the reactive flux going back non-negligible.

We can give a similar explanation in the case of F^+ and $Cl^+ + H_2O$ reactions. The triplet and singlet potential energy surfaces for both reactions have been studied in Refs. [24] and [25] respectively. Here we will assume that reactions occur on the ground (triplet) state. In Fig. 2 we show a simplified scheme of these surfaces in which we have omitted those stationary points that are not relevant to this work.

The $F^+ + H_2O$ reaction is extremely exothermic. The products corresponding to the charge transfer process are predicted to be 109.7 kcal/mol below the reactants. Other possible products ($OH + HF^+$ and $OH^+ + HF$)

Fig. 2. Energetic profile for the $F^+(^3P) + H_2O$ and $Cl^+(^3P) + H_2O$ reaction paths
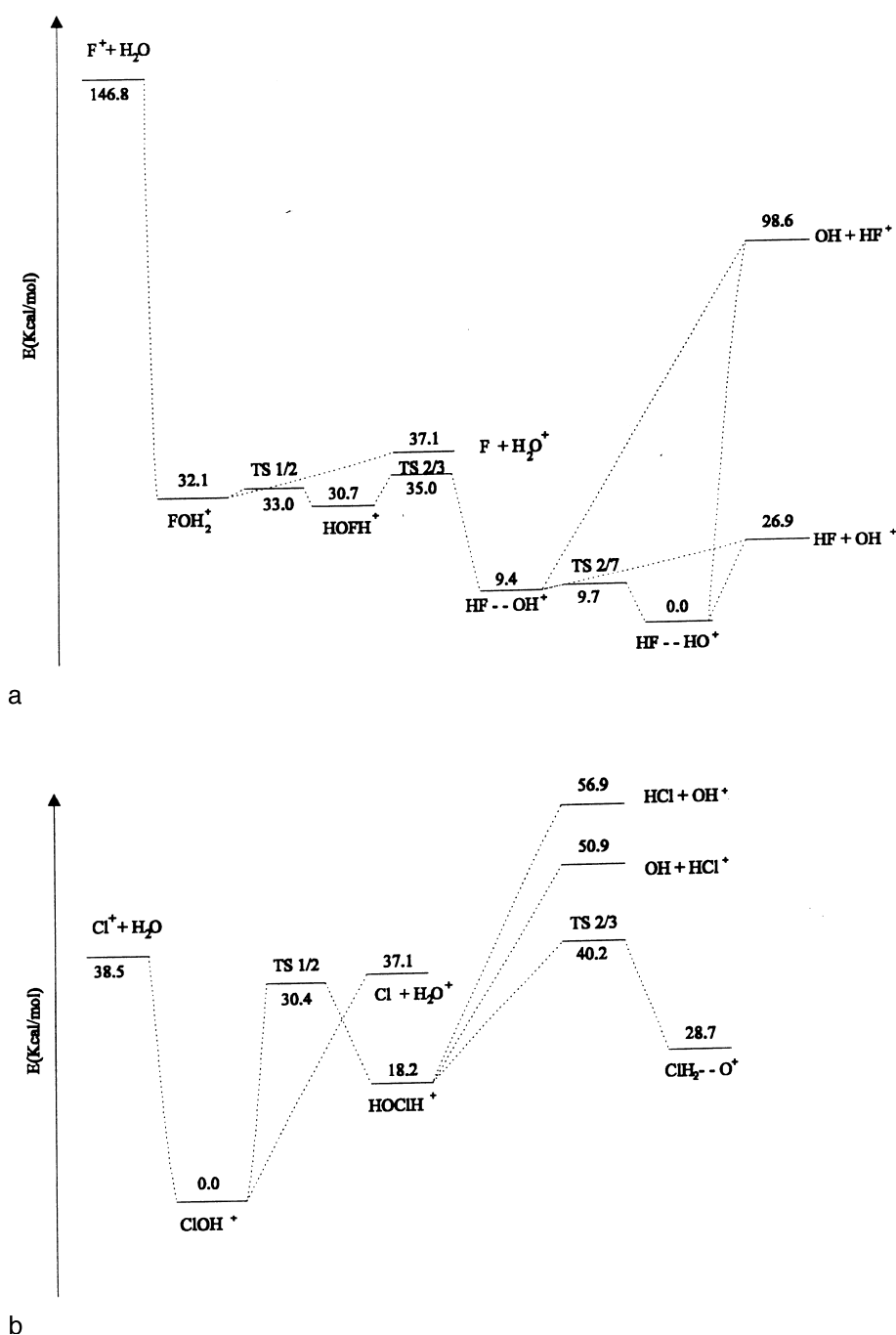
are also found considerably below reactants (48.2 and 119.9 kcal/mol). The path between reactants and products goes through different isomers, all of them energetically accessible with barriers far below the entrance channel. The $Cl^+ + H_2O$ reaction is very different. Here the only possible products of reaction are $H_2O^+ + Cl$, due to the presence of barriers higher in energy than reactants that prevent dissociation into other products. The charge transfer products are only at -5.0 kcal/mol below the reactants, i.e. the reaction is only slightly exothermic. Then, once again, the application of capture theory is more questionable.

In general we see that reactions which involve second row monocations are less suitable for application of the capture approximation. If we exclude $N^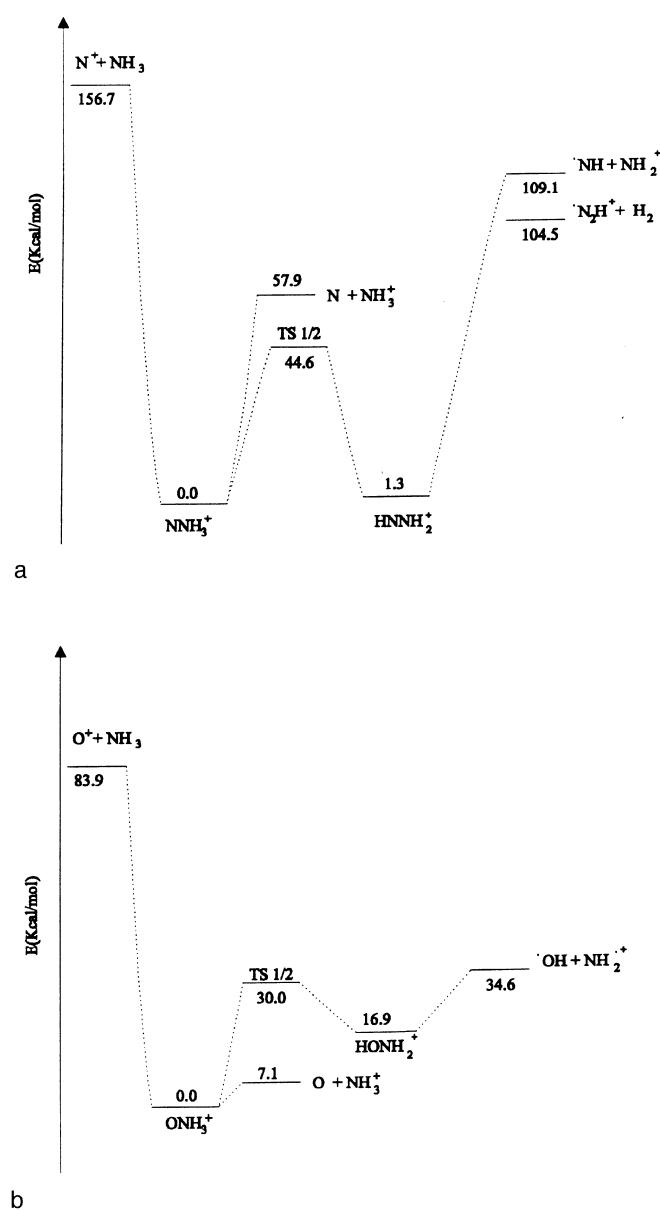+ + HCOOH$ and $O^+ + HCOOH$ reactions for the reasons given above, we find that over 80% of reactions of the first row cations considered yield an agreement between our theoretical estimation and the experimental rate constant within 20% . However, this agreement is only reached for 35% of reactions involving second row cations. This clearly corresponds to the smaller electronegativity of this species compared with their corresponding first row analogs. The first row cations bear much better the deficiency of electronic charge and the energy released is smaller for second row cations. Hence this energy might not be enough to overcome subsequent barriers and reflection of the reactive flux may not be discarded.

However there are other cases in which discrepancies between experiment and theory are not well understood. For instance, we found it interesting to investigate the $O^+ + NH_3$ reaction. We have chosen the $N^+ + NH_3$ reaction for comparison with this system as it is a very similar reaction for which we have found a good agreement (within 8%) between theory and experiment. In a previous ab initio study on the $N^+ + NH_3$ reaction, the ground and excited states have been described [26]. However, we found serious discrepancies with this study as far as the relative stabilities of the different stationary points of the Potential Energy Surface (PES) are concerned. Hence, we consider it worth including our calculations here (see Fig. 3). Details of geometric parameters and other properties of the different structures are available upon request.

In Fig. 3a we show the reaction profile for the $N^+ + NH_3$ reaction. The first step corresponding to the formation of the adduct was reported in Ref. [26] to be 201.5 kcal/mol exothermic. Our estimations predict a much smaller value (156.7 kcal/mol). This large difference is very unlikely to be a consequence of the improvement in the level of theory.

This complex could evolve to yield the charge transfer products, situated at 57.9 kcal/mol or through the transition structure TS 1/2 to yield the insertion of the nitrogen atom into one of the N—H bonds. From this latter isomer the dissociation into fragments $NH_2^+ + NH$ was predicted in Ref. [26] to happen through a new transition state. This is a surprising result as a charge-dipole interaction is expected to take place without an energetic barrier. We have found that the structure proposed in the aforementioned reference is a saddle point with two imaginary frequencies rather than a transition state, even when the optimization is carried out at the $MP2/6-31 + G(D,P)$ level in order to include correlation effects and diffuse functions in the basis set.[1] Therefore we must conclude that the $HNNH_2^+$ complex dissociates to $NH_2^+ + NH$ without an activation barrier.

The profile of the $O^+ + NH_3$ reaction is basically rather similar to the previous one (see Fig. 3b); once again the first step is the formation of an adduct that could evolve with no barrier to the charge transfer products or through the transition state TS 1/2 to the insertion complex that would eventually yield the corresponding fragments, $OH + NH_2^+$. However in this case charge transfer is a much more competitive process as

Fig. 3. Energetic profile for the $N^+(^3P) + NH_3$ and $O^+(^4S) + NH_3$ reaction paths

[1] The optimized structures in Ref. [23] were calculated at UHF/6-31G**

Fig. 4. Energetic profile for the $F^+(^3P) + H_2S$ reaction path
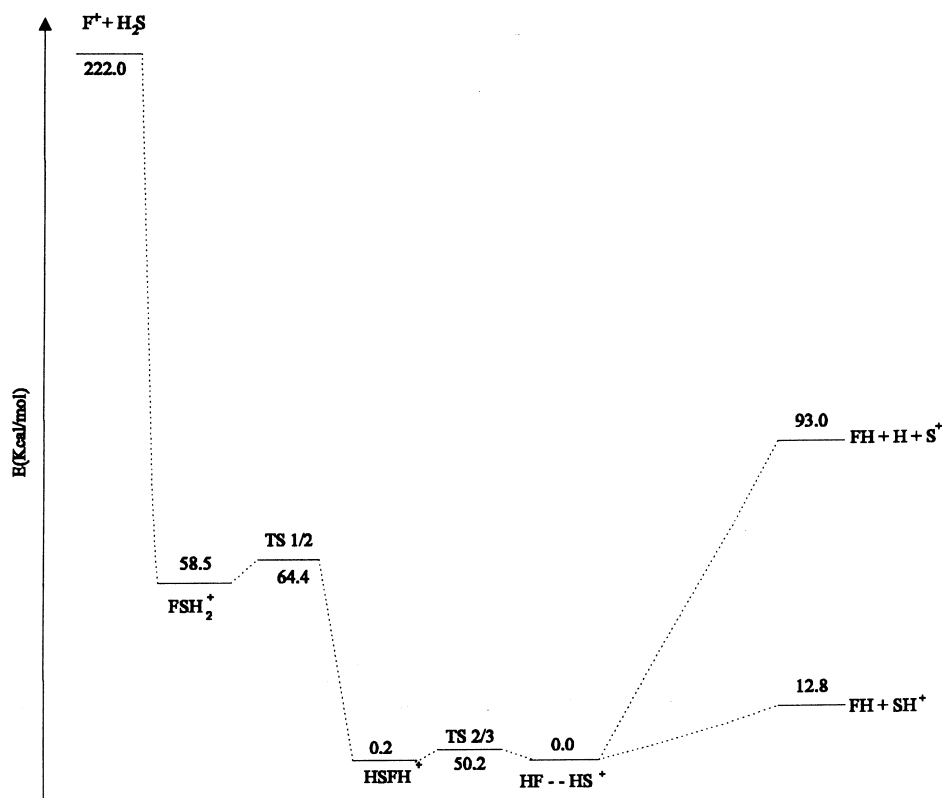
$O + NH_3^+$ products are only 7.1 kcal/mol above the adduct, while evolution to the insertion complex has a barrier of 30.0 kcal/mol. This fact agrees with experimental evidence that shows that while for the $N^+ + NH_3$ reaction the fragments $NH + NH_2^+$ are detected (20%), for $O^+ + NH_3$ the only products detected are those corresponding to the charge transfer process.

The $O^+ + NH_3$ reaction profile is, in principle, thermodynamically appropriate for application of the capture approximation in the sense that it is sufficiently exothermic. The fact that experimentally this reaction is slower than predicted is not well understood and needs further attention.

The case of the $F^+ + H_2S$ reaction is rather peculiar. This is probably the most exothermic of all reactions we are dealing with. A simplified scheme of this reaction profile is given in Fig. 4 (taken from Ref. [27]); we have only eliminated those enantiomeric structures that are not relevant from the energetic point of view. It is quite surprising that the estimated rate constant is significantly higher than the experimental one. In contrast, for its analogous reaction $Cl^+ + H_2S$ the agreement found between theory and experiment is good. Unfortunately, there is no information about the hypersurface of the $Cl^+ + H_2S$ reaction but very probably the effect of the minor electronegativity of the Cl^+ cation with respect to F^+ will make this reaction much less exothermic and therefore with more significant secondary barriers in the reaction path. Hence the reasons why the $F^+ + H_2S$ reaction is much slower than predicted are not evident, mainly if one takes into account that the energetics of the corresponding potential energy surface would indicate this reaction to be one of the most suitable examples for the application of capture approximation.

4 Conclusions

The ACCSA method has been applied to 35 reactions of first and second row monocations with different neutrals. The predictions of global rate constants at 300 K are in good agreement with experimental measurements for the 80% of reactions involving first row cations but only for 35% in the case of second row cations. The systems for which the prediction fails usually correspond to situations in which the reaction is not very exothermic or secondary barriers are present in the reaction path. This violates application of capture theory. Therefore using this method as a first approach to obtain theoretical values for rate coefficients in dipolar molecule-ion reactions must be done carefully. This is especially the case when the ion involved is a second row atom since the smaller electronegativity increases the height of secondary barriers in the potential energy surface. In spite of this, there are some reactions involving second row monocations for which the ACCSA method predicts rate constants that agree very well with experimental data. However, a preliminary exploration of the energetics of reaction profile may be very useful in determining if the reaction is suitable for the application of capture theory.

References

1. Armentrout PB, Baer T (1996) J Phys Chem 100:12866 and references therein
2. Duley WW, Williams DA (1984) Interstellar chemistry. Academic Press, London
3. (a) Maier JP, Thommen F (1982) J Chem Phys 77:4427; (b) Polak M. Gruebele M, DeKock BW, Saykally RJ (1989) Mol Phys 66:1193
4. (a) Knott WJ, Proch D, Kompa KL, Rose-Petruck C (1995) J Chem Phys 102:214; (b) Uiterwaal CJGJ, van Eck J, Niehaus A (1995) J Chem Phys 102:744
5. (a) Walker RB, Light JC (1980) Annu Rev Phys Chem 31:401; (b) Connor JNL (1979) Comput Phys Commun 17:117; (c) Baer M (1982) Adv Chem Phys 49:191
6. Clary DC (1990) Annu Rev Phys Chem 41:61
7. See for instance: (a) Tröe J (1986) J Phys Chem 90:3485; (b) Tröe J (1987) J Chem Phys 87:2773; (c) Bates DR, Morgan WL (1987) J Chem Phys 87:2611; (d) Su T, Chesnavich WJ (1982) J Chem Phys 76:5183
8. Clary DC (1984) Mol Phys 53:3
9. Clary DC (1985) Mol Phys 54:605
10. Clary DC (1987) J Chem Soc Faraday Trans II 83:139
11. Dateo CE, Clary DC (1989) J Chem Phys 90:7216
12. Clary DC (1995) Chem Phys Lett 232:267
13. Clary DC, Smith D, Adams NG (1985) Chem Phys Lett 119:320
14. Curtiss LA, Raghavachari K, Trucks GW, Pople JA (1991) J Chem Phys 94:7221
15. Frisch MJ, Trucks GW, Schlegel HB, Gill PMW, Johnson BG, Robb MA, Cheeseman JR, Keith TA, Peterson GA, Montgomery JA, Raghavachari K, Al-Laham MA, Zakrzewski VG, Ortiz JV, Foresman JB, Cioslowski J, Stefanow BB, Nanayaklara A, Challacombe M, Peng CY, Ayala PY, Chen W, Wong MW, Andres JL, Replogle ES, Gomperts R, Martin RL, Fox DJ, Binkley JS, Defrees DJ, Baker J, Stewart JP, Head-Gordon M, Gonzalez C, Pople JA (1995) Gaussian 94. Gaussian, Inc., Pittsburgh, Pa
16. Handbook of chemistry and physics, 64th edn (1984) CRC Press, Boca Raton
17. Anicich VG (1993) J Phys Chem Ref Data 22:1469
18. Clary DC, Dateo CE, Smith D (1990) Chem Phys Lett 167:1
19. Flores JR, Redondo P, Azpeleta S (1995) Chem Phys Lett 240:193
20. Hrusak J, Bohme DK, Wlodek S, Schwarz H (1992) J Phys Chem 96:5355
21. Bouma JW, Burgers PC, Holmes JL, Radom L (1986) J Am Chem Soc 108:1767
22. Ma NL, Smith BJ, Pople JA, Radom L (1991) J Am Chem Soc 113:7903
23. Flores R, Redondo P (1994) Chem Phys Lett 230:358
24. Luna A, Manuel M, Mó O, Yáñez M (1994) J Phys Chem 98:6980
25. Manuel M, Mó O, Yáñez M (1997) J Phys Chem 101:1722
26. Song Y (1993) J Mol Struct 283:268
27. Manuel M, Mó O, Yáñez M (1997) Mol Phys 91:503